Progress In Electromagnetics Research, Vol. 123, 407–426, 2012

NEW WILKINSON POWER DIVIDERS BASED ON COMPACT STEPPED-IMPEDANCE TRANSMISSION LINES AND SHUNT OPEN STUBS

P.-H. Deng*, J.-H. Guo, and W.-C. Kuo

Department of Electrical Engineering, National University of Kaohsiung, No. 700, Kaohsiung University Road, Nan-Tzu District, Kaohsiung 811, Taiwan

Abstract—This study presents new Wilkinson power dividers using compact stepped-impedance structures and capacitive loads to achieve the required power splitting. This approach can produce additional transmission zeros and effectively suppress the desired stopbands because shunt open stubs realize capacitive loads. This study proposes two equal-split dividers and two unequal-split dividers. For the first equal-split case, one shunt open stub forms the needed capacitor in each transmission path, creating one additional transmission zero in each path. To obtain one more transmission zero in each transmission path, the second Wilkinson power divider uses two shunt open stubs in each path to achieve the same capacitor value as the first divider. This study also tests unequal-split dividers with one and two transmission zeros in each path to confirm that compact stepped-impedance transmission lines and shunt-to-ground capacitors can be utilized in unequal power division.

1. INTRODUCTION

Conventional Wilkinson power dividers [1] are often used for power division in microwave communication systems because they have high isolation between arbitrary two output ports, low transmission loss in each channel, and a simple fabrication procedure. However, there are some obstacles to conventional circuit design, such as large circuit occupation, achieving multi-band response, and poor stopband rejections. Therefore, several researchers [1–44] have discussed how to improve the conventional Wilkinson power dividers.

Received 16 November 2011, Accepted 26 December 2011, Scheduled 4 January 2012

* Corresponding author: Pu-Hua Deng (phdeng@nuk.edu.tw).

One of the main problems in the conventional Wilkinson power divider [1] is that it uses two quarter-wavelength ($\lambda/4$) transmission lines in each transmission path, resulting in a large circuit size. Replacing these $\lambda/4$ transmission lines with different architectures [2–10] makes them possible to achieve small circuit sizes.

Researchers have proposed several types of power dividers [11–25] to satisfy the different requirements for dual-band applications. One configuration [12] attaches two central transmission line stubs to a conventional Wilkinson power divider for dual-band responses. Another approach [13] uses a power divider with artificial transmission lines for a compact dual-band application. The structure [17] uses two sections of non-uniform transmission line transformers to create a miniaturized dual-band divider.

Many studies [26–30] present dividers with harmonic suppression. One design [26] replaces the quarter-wavelength ($\lambda/4$) transmission lines in the conventional Wilkinson power divider with a pair of coupled-lines on a defected ground structure (DGS) for effective harmonic suppression. A microstrip power divider [27] with two open stubs at the center of the $\lambda/4$ transmission lines can achieve harmonic suppression.

The constant VSWR-type three-port 3-dB power divider (CVT3PD) in [31] consists of one perfect isolation circuit between two output ports. This design uses stepped-impedance transmission lines in each transmission path to achieve a small circuit size.

The current study proposes a design in which two new equal-split and two unequal-split Wilkinson power dividers replace the $\lambda/4$ branches of the conventional Wilkinson power dividers with compact stepped-impedance transmission line sections. Although the CVT3PD [31] uses similar stepped-impedance transmission line sections to reduce the circuit size, the proposed dividers employ shunt-to-ground capacitors that are unlike the series capacitor in the CVT3PD isolation circuit. The perfect isolation circuit in CVT3PD requires a series capacitor which may be realized by several types of capacitors such as a chip capacitor, gap capacitor, and planar interdigital capacitor. However, these capacitors may introduce the discontinuity effect and parasitic effect, which are difficult to control. Unlike the series capacitor in CVT3PD, the shunt-to-ground capacitors in the proposed dividers can be formed easily by planner open stubs. With the appropriate lengths, these stubs can create additional transmission zeros to improve the required band rejections. The proposed equal- and unequal-split Wilkinson power dividers can decide all the design parameters by analyzing the even- and odd-mode equivalent circuits.

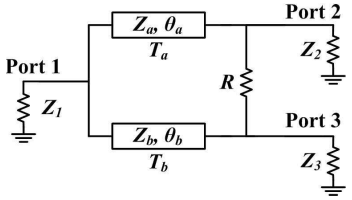

Figure 1. Conventional Wilkinson power divider [1].

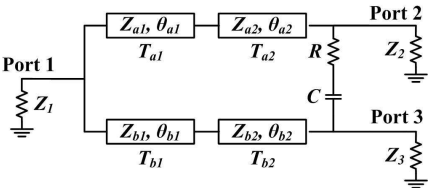

Figure 2. Constant VSWR-type three-port 3-dB power divider (CVT3PD) [31].

2. COMPARING THE PROPOSED POWER DIVIDER WITH PREVIOUS WORKS

Figure 1 shows that a conventional Wilkinson power divider [1] consists of two $\lambda/4$ transmission lines (T_a and T_b) and an isolation resistor R. The two $\lambda/4$ transmission lines (T_a and T_b) usually occupy a large circuit area. Therefore, to reduce the lengths of $\lambda/4$ transmission lines, the constant VSWR-type three-port 3-dB power divider (CVT3PD) structure [31] uses stepped impedance transmission line sections. In this design, transmission lines T_{a1} and T_{a2} or transmission lines T_{b1} and T_{b2} have different characteristic impedances, and a resistor R may be connected in series with a capacitor C between two output ports (Figure 2). Here, the capacitor C can be implemented by a chip capacitor or planar microwave lumped capacitor (e.g., interdigital capacitor or gap capacitor). However, these capacitors may introduce the discontinuity effect and parasitic effect, respectively. This study presents a new type of Wilkinson power divider (Figure 3) to overcome this problem. In Figure 3, Z_{ai}/Z_{bi} and θ_{ai}/θ_{bi}, $i = 1$, or 2, are the characteristic impedance and electrical length of the transmission line, respectively. Compared Figure 3 with Figure 2, the proposed structure (Figure 3) utilizes two shunt-to-ground capacitors C_1 and C_2, which can be realized easily by distributed components (e.g., shunt open stubs). This approach avoids the series capacitor C in Figure 2. Similar even-odd mode analyses of conventional Wilkinson power dividers [1] and [34] can obtain the related design equations of the proposed divider (Figure 3).

3. DESIGN OF THE PROPOSED EQUAL-SPLIT WILKINSON POWER DIVIDER

Figure 4 shows the proposed equal-split (3-dB) Wilkinson power divider configuration. Each part is symmetric across the midplane and

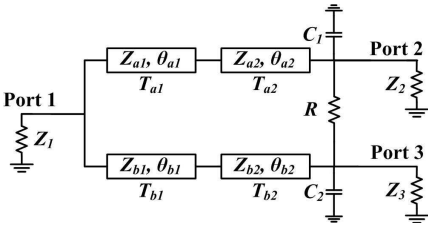

Figure 3. The proposed Wilkinson power divider.

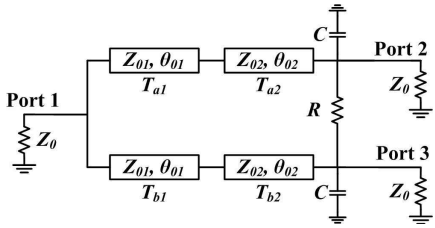

Figure 4. Proposed equal-split (3-dB) Wilkinson power divider.

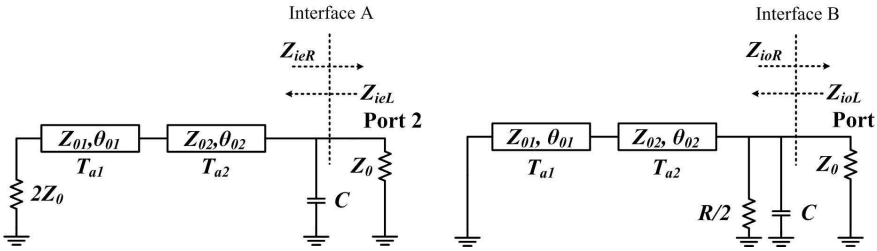

(a) (b)

Figure 5. (a) Even-mode and (b) odd-mode equivalent circuits for the proposed equal-split (3-dB) Wilkinson power divider.

the termination resistor for each port is set to be the system impedance Z_0, that is, $Z_{a1} = Z_{b1} = Z_{01}$, $\theta_{a1} = \theta_{b1} = \theta_{01}$, $Z_{a2} = Z_{b2} = Z_{02}$, $\theta_{a2} = \theta_{b2} = \theta_{02}$, $C_1 = C_2 = C$, and $Z_1 = Z_2 = Z_3 = Z_0$ in Figure 3. Figure 5 shows the equivalent circuits of the upper side for even- and odd-mode excitations. Here, the analysis of each mode selects the upper side because the upper- and the lower-side equivalent circuits of each mode are the same.

In Figure 5(a) (even-mode equivalent circuit), the impedances (Z_{ieL} and Z_{ieR}) looking into both sides must be equal at the interface A for matching requirement. The resulting equation can be written as

$$Z_0 = \left\{ \frac{1}{\left[Z_{02} \left(\frac{Z_{ie} + jZ_{02} \tan\theta_{02}}{Z_{02} + jZ_{ie} \tan\theta_{02}} \right) \right]} + j\omega C \right\}^{-1} \tag{1}$$

where

$$Z_{ie} = Z_{01} \left(\frac{2Z_0 + jZ_{01} \tan\theta_{01}}{Z_{01} + j2Z_0 \tan\theta_{01}} \right).$$

In Equation (1), ω is the radian frequency. Rearranging and separating the real and imaginary parts of Equation (1) lead to Equations (2a)

and (2b):

$$\begin{aligned} & Z_{01}Z_{02} + \left(Z_{01}^2 - 2Z_{02}^2\right)\tan\theta_{01}\tan\theta_{02} \\ = \; & -\omega C Z_{01}Z_{02}\left(Z_{01}\tan\theta_{01} + Z_{02}\tan\theta_{02}\right) \end{aligned} \tag{2a}$$

$$\begin{aligned} & Z_{01}^2 Z_{02}\tan\theta_{01} + Z_{01}Z_{02}^2\tan\theta_{02} \\ = \; & 2Z_0^2\omega C Z_{02}\left(Z_{01} - Z_{02}\tan\theta_{01}\tan\theta_{02}\right) \\ & +2Z_0^2\left(Z_{02}\tan\theta_{01} + Z_{01}\tan\theta_{02}\right). \end{aligned} \tag{2b}$$

Similarly, in Figure 5(b) (odd-mode equivalent circuit), the impedances (Z_{ioL} and Z_{ioR}) looking into both sides must be the same at the interface B for matching requirement. This equation can be written as

$$Z_0 = \left(\frac{1}{Z_{io}} + \frac{2}{R} + j\omega C\right)^{-1} \tag{3}$$

where

$$Z_{io} = jZ_{02}\left(\frac{Z_{01}\tan\theta_{01} + Z_{02}\tan\theta_{02}}{Z_{02} - Z_{01}\tan\theta_{01}\tan\theta_{02}}\right).$$

Rearranging and separating the real and imaginary parts of Equation (3) lead to Equations (4a) and (4b):

$$R = 2Z_0 \tag{4a}$$

$$\omega C = \frac{Z_{02} - Z_{01}\tan\theta_{01}\tan\theta_{02}}{Z_{01}Z_{02}\tan\theta_{01} + Z_{02}^2\tan\theta_{02}}. \tag{4b}$$

Equations (2a), (2b), (4a), and (4b) can calculate all of the design parameters in Figure 3. To obtain an arbitrary power division, the following section introduces the design of the proposed unequal-split Wilkinson power divider.

4. DESIGN OF THE PROPOSED UNEQUAL-SPLIT WILKINSON POWER DIVIDER

The proposed unequal-split Wilkinson power divider (Figure 3) can also be simplified its analysis by the even- and odd-mode equivalent circuits, as suggested by [34] and shown in Figure 6. When each equivalent circuit in Figure 6 exhibits impedance matching at the interfaces A, B, C, or D, the design equations from Figure 6 can be derived. In Figure 6(a) (upper side even-mode equivalent circuit), the impedances (Z_{ieLx} and Z_{ieRx}) looking into both sides must be equal

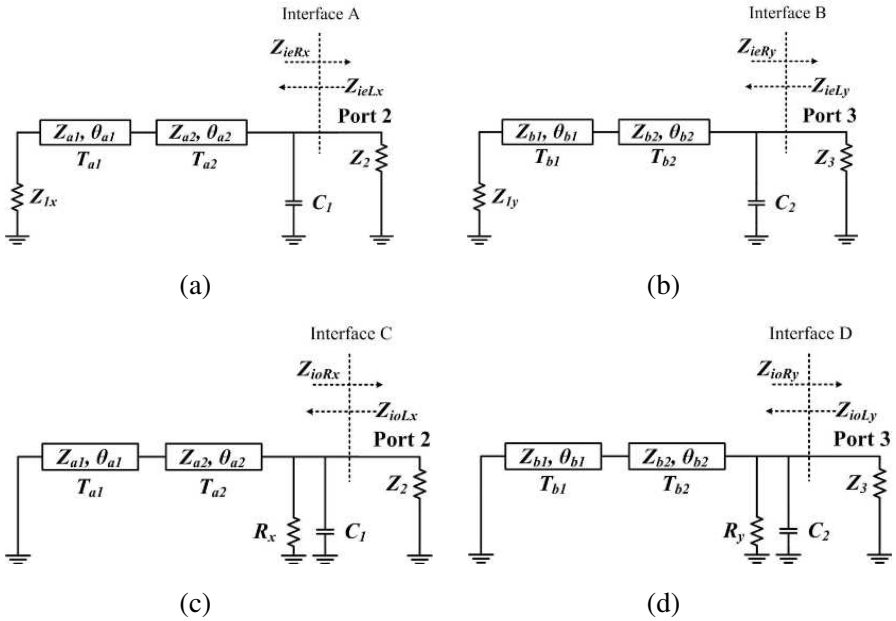

Figure 6. (a) Upper side even-mode, (b) lower side even-mode, (c) upper side odd-mode, and (d) lower side odd-mode equivalent circuits for the proposed unequal-split Wilkinson power divider.

at the interface A for matching requirement. The resulting equation can be written as

$$\begin{aligned} & (Z_{1x} - Z_2)\, Z_{a1} Z_{a2} + \left(Z_2 Z_{a1}^2 - Z_{1x} Z_{a2}^2\right) \tan\theta_{a1} \tan\theta_{a2} \\ = \; & -\omega C_1 Z_{a1} Z_{a2} Z_2 \left(Z_{a1} \tan\theta_{a1} + Z_{a2} \tan\theta_{a2}\right) \qquad (5a) \\ & Z_{a1}^2 Z_{a2} \tan\theta_{a1} + Z_{a1} Z_{a2}^2 \tan\theta_{a2} \\ = \; & Z_{1x} Z_2 \omega C_1 Z_{a2} \left(Z_{a1} - Z_{a2} \tan\theta_{a1} \tan\theta_{a2}\right) \\ & + Z_{1x} Z_2 \left(Z_{a2} \tan\theta_{a1} + Z_{a1} \tan\theta_{a2}\right). \qquad (5b) \end{aligned}$$

In Figure 6(b) (lower side even-mode equivalent circuit), the impedances (Z_{ieLy} and Z_{ieRy}) looking into both sides must be equal at the interface B for matching requirement. The resulting equation can be written as

$$\begin{aligned} & (Z_{1y} - Z_3)\, Z_{b1} Z_{b2} + \left(Z_3 Z_{b1}^2 - Z_{1y} Z_{b2}^2\right) \tan\theta_{b1} \tan\theta_{b2} \\ = \; & -\omega C_2 Z_{b1} Z_{b2} Z_3 \left(Z_{b1} \tan\theta_{b1} + Z_{b2} \tan\theta_{b2}\right) \qquad (6a) \\ & Z_{b1}^2 Z_{b2} \tan\theta_{b1} + Z_{b1} Z_{b2}^2 \tan\theta_{b2} \\ = \; & Z_{1y} Z_3 \omega C_2 Z_{b2} \left(Z_{b1} - Z_{b2} \tan\theta_{b1} \tan\theta_{b2}\right) \\ & + Z_{1y} Z_3 \left(Z_{b2} \tan\theta_{b1} + Z_{b1} \tan\theta_{b2}\right). \qquad (6b) \end{aligned}$$

In Figure 6(c) (upper side odd-mode equivalent circuit), the impedances (Z_{ioLx} and Z_{ioRx}) looking into both sides must be equal at the interface C for matching requirement. The resulting equation can be written as

$$Z_2 = R_x \tag{7a}$$

$$\omega C_1 = \frac{Z_{a2} - Z_{a1} \tan\theta_{a1} \tan\theta_{a2}}{Z_{a1} Z_{a2} \tan\theta_{a1} + Z_{a2}^2 \tan\theta_{a2}}. \tag{7b}$$

In Figure 6(d) (lower side odd-mode equivalent circuit), the impedances (Z_{ioLy} and Z_{ioRy}) looking into both sides must be equal at the interface D for matching requirement. The resulting equation can be written as

$$Z_3 = R_y \tag{8a}$$

$$\omega C_2 = \frac{Z_{b2} - Z_{b1} \tan\theta_{b1} \tan\theta_{b2}}{Z_{b1} Z_{b2} \tan\theta_{b1} + Z_{b2}^2 \tan\theta_{b2}}. \tag{8b}$$

In conventional unequal-split Wilkinson power divider [34], the power ratio of Port 2 to Port 3 (k^2), which is used in the proposed unequal-split power divider, can be written as

$$k^2 = Z_3/Z_2 = Z_{1y}/Z_{1x} = R_y/R_x. \tag{9}$$

Besides, from the Figure 3 and the Figure 6 (the even- and odd-mode analyses of Figure 3), the resistor R and Z_1 can be written as

$$R = R_x + R_y \tag{10}$$

$$Z_1 = Z_{1x}//Z_{1y}. \tag{11}$$

Therefore, Equations (5a), (5b), 6(a), 6(b), 7(a), 7(b), 8(a), 8(b), (9), (10), and (11) can be used to calculate all the design parameters in Figure 3.

5. IMPLEMENTING THE PROPOSED EQUAL-SPLIT POWER DIVIDERS

The proposed Wilkinson power divider (Figure 3) consists of two shunt-to-ground capacitors for equal-split or unequal-split power division, as introduced in Sections 3 and 4. Although two shunt-to-ground capacitors can use chip capacitors, they may produce unexpected discontinuity. To avoid this effect and create additional transmission zeros at unwanted frequencies, shunt microstrip open stubs can be used to form capacitors in the proposed configuration. The shunt-to-ground capacitor C is equivalent to several shunt-to-ground capacitors (C_{n1}, C_{n2}, ..., C_{ni}) or several open stubs (*Stub 1*, *Stub 2*, ..., *Stub n*) in

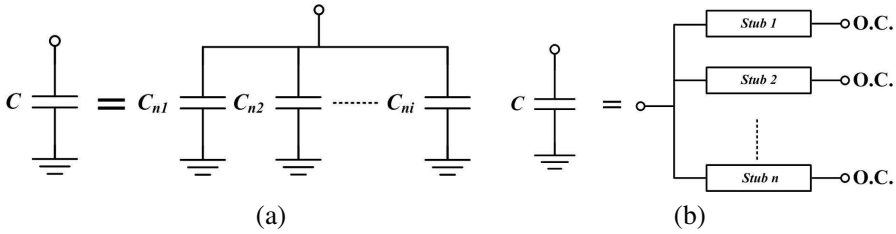

Figure 7. Equivalent circuits of (a) a shunt-to-ground capacitor with several capacitors in parallel and (b) a shunt-to-ground capacitor with several open stubs in parallel.

parallel (Figure 7). This means that several transmission zeros can be produced to improve the rejection levels in the desired stopbands. The design steps for the proposed equal-split Wilkinson power divider can be summarized as follows.

Step 1) All of the design parameters in Figure 4 can be determined by Equations (2a), (2b), (4a), and (4b).

Step 2) Decide the required rejection frequencies of each transmission path which can be achieved by using several open stubs (*Stub 1*, *Stub 2*, ..., *Stub n*) in parallel (Figure 7) to realize the shunt-to-ground capacitor C of each transmission path in Figure 4.

This study presents two equal-split and two unequal-split Wilkinson power dividers to demonstrate this concept. The first equal-split Wilkinson power divider uses one shunt open stub to create an additional transmission zero to improve the stopband rejection and realize the shunt-to-ground capacitor near each output port (Figure 8).

Equations (2a), (2b), (4a), and (4b) can calculate the required design parameters for the proposed equal-split power divider. Here, the center frequency of the divider is 2 GHz and one of the solutions is selected as the system impedance $Z_0 = 50\,\Omega$, resistor $R = 100\,\Omega$, shunt-to-ground capacitor $C = 0.75\,\text{pF}$, characteristic impedances $Z_{01} = 43.03\,\Omega$ and $Z_{02} = 129.3\,\Omega$, and the electrical lengths $\theta_{01} = 32.7^\circ$ and $\theta_{02} = 27.4^\circ$. The sum of the electrical lengths θ_{01} and θ_{02} in the proposed equal-split power divider is approximately 33.3% shorter than the $\lambda/4$ transmission line in the conventional equal-split Wilkinson power divider (Figure 1).

As mentioned above, the shunt-to-ground capacitor is substituted by the open stub to produce additional transmission zero in each transmission path to improve the required stopband level. All of the dividers in this study were implemented on a substrate with a relative dielectric constant of 4.4, a thickness of 1.6 mm, and a loss tangent of 0.02. Figure 9 shows the layout of the proposed equal-split power

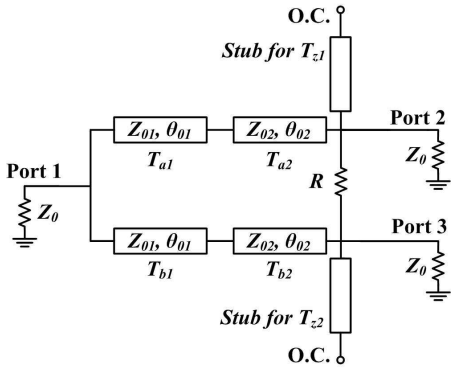

Figure 8. The equal power divider with one shunt open stub near each output port.

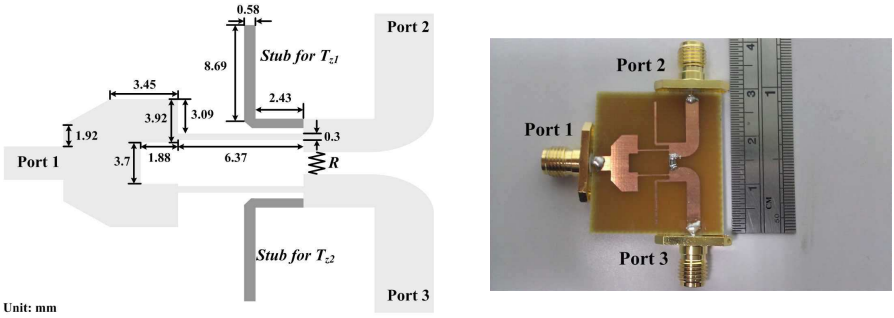

(a) (b)

Figure 9. (a) Layout and (b) photograph of the proposed equal-split power divider with one shunt open stub in each transmission path.

divider with one additional transmission zero in each transmission path. Here, the length of the stub in each transmission path is approximately $\lambda/4$ at 4 GHz, creating one additional transmission zero (T_{z1} or T_{z2}) around 4 GHz. Figure 10 presents the measured and simulated scattering parameters ($|S_{11}|$, $|S_{21}|$, $|S_{31}|$, and $|S_{32}|$) of the proposed power divider (Figure 9). The measured result of the minimal insertion loss in each transmission path is 3.407 dB ($|S_{21}|$ or $|S_{31}|$). The measured maximal isolation ($|S_{32}|$) between two output ports is 33.51 dB. This design also exhibits a favorable rejection level of $|S_{21}|$ or $|S_{31}|$ at approximately 4 GHz because there is one shunt open stub near each output port.

Figure 11 shows the second equal-split Wilkinson power divider configuration. All the design parameters and the center frequency

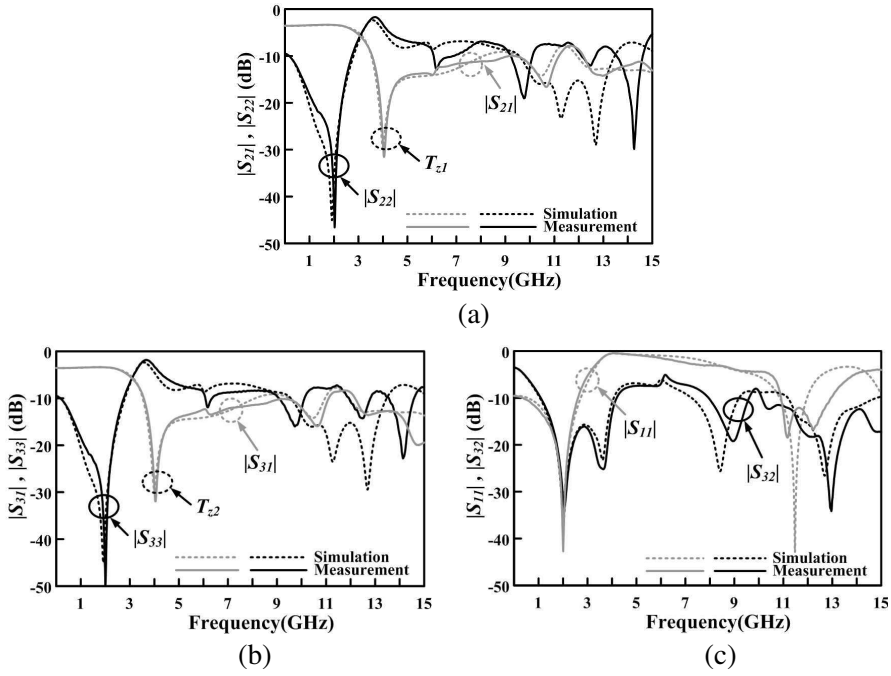

Figure 10. The measured and simulated scattering parameters of the proposed power divider in Figure 9. (a) $|S_{21}|$ and $|S_{22}|$. (b) $|S_{31}|$ and $|S_{33}|$. (c) $|S_{11}|$ and $|S_{32}|$.

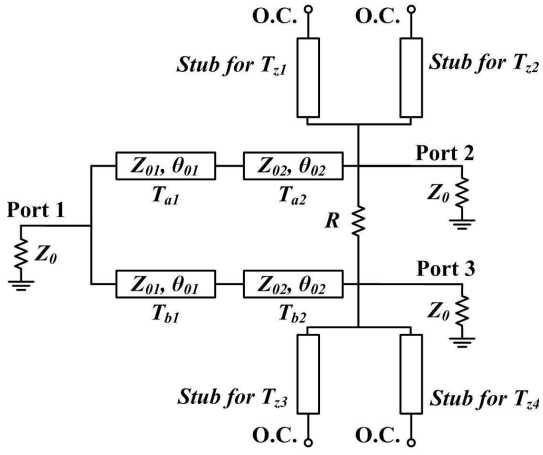

Figure 11. The equal power divider with two shunt open stubs near each output port.

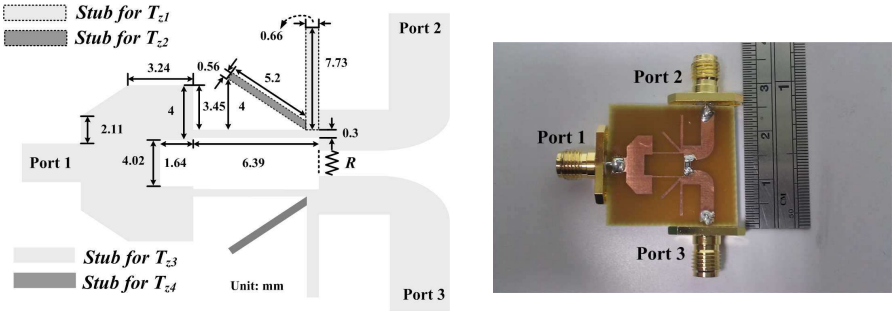

Figure 12. (a) Layout and (b) photograph of the proposed equal-split power divider with two shunt open stubs in each transmission path.

are the same as the first equal-split case (Figure 8) except for the implementing approach of shunt-to-ground capacitor near each output. The difference here is that the second equal-split Wilkinson power divider uses two shunt open stubs in each path. Using two shunt open stubs creates two additional transmission zeros in each path, and each of them can be designed at the desired rejection frequency independently by adjusting the length and the characteristic impedance of each shunt open stub. Figure 12 shows the layout of the proposed equal-split power divider with two additional transmission zeros in each transmission path. The lengths of the shunt open stubs in each transmission path are approximately $\lambda/4$ at 6 GHz and 8 GHz, respectively. These create two additional transmission zeros T_{z1}/T_{z3} and T_{z2}/T_{z4} at approximately 6 GHz and 8 GHz, respectively. Figure 13 presents the measured and simulated scattering parameters ($|S_{11}|$, $|S_{21}|$, $|S_{31}|$, and $|S_{32}|$) of the proposed power divider (Figure 12). The measured minimal insertion loss in each transmission path is 3.36 dB ($|S_{21}|$ or $|S_{31}|$). The measured maximal isolation ($|S_{32}|$) between two output ports is 31.46 dB. There are remarkable rejection responses of $|S_{21}|$ and $|S_{31}|$ at approximately 6 GHz and 8 GHz, respectively, because each output port includes two shunt open stubs.

6. IMPLEMENTING THE PROPOSED UNEQUAL-SPLIT POWER DIVIDERS

The design steps for the proposed unequal-split Wilkinson power divider can also be summarized as follows.

Step 1) All of the design parameters in Figure 3 can be determined by Equations (5a), (5b), 6(a), 6(b), 7(a), 7(b), 8(a), 8(b), (9), (10),

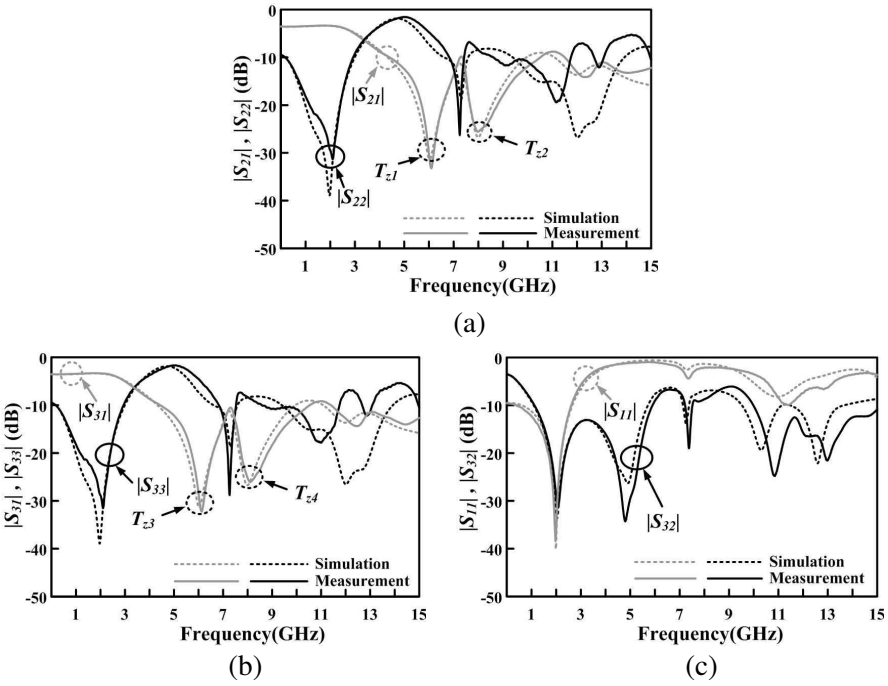

Figure 13. The measured and simulated scattering parameters of the proposed power divider in Figure 12. (a) $|S_{21}|$ and $|S_{22}|$. (b) $|S_{31}|$ and $|S_{33}|$. (c) $|S_{11}|$ and $|S_{32}|$.

and (11).

Step 2) Decide the required rejection frequencies of each transmission path which can be achieved by using several open stubs (*Stub 1*, *Stub 2*, ..., *Stub n*) in parallel (Figure 7) to realize the shunt-to-ground capacitors C_1 and C_2 in Figure 3.

To demonstrate one unequal circuit, the specification about the power ratio of Port 2 to Port 3 (k^2) is 3/2, the center frequency is 2 GHz, and one of the solutions in Figure 6 is selected as $Z_{1x} = 83.3\,\Omega$, $Z_{1y} = 125\,\Omega$, $Z_1 = 50\,\Omega$, $R = 100\,\Omega$, $Z_{a1} = 36.01\,\Omega$, $\theta_{a1} = 35.4^\circ$, $Z_{a2} = 126.7\,\Omega$, $\theta_{a2} = 21.8^\circ$, $C_1 = 0.96\,\text{pF}$, $Z_2 = 40\,\Omega$, $Z_3 = 60\,\Omega$, $Z_{b1} = 46.46\,\Omega$, $\theta_{b1} = 25.3^\circ$, $Z_{b2} = 129.5\,\Omega$, $\theta_{b2} = 37.2^\circ$, and $C_2 = 0.58\,\text{pF}$. To form a shunt-to-ground capacitor (C_1 or C_2) in each transmission path, using the shunt open stub creates additional transmission zero to improve the stopband rejection level in each desired frequency. Figure 14 shows the proposed unequal power divider with one shunt open stub in each transmission path, forming the

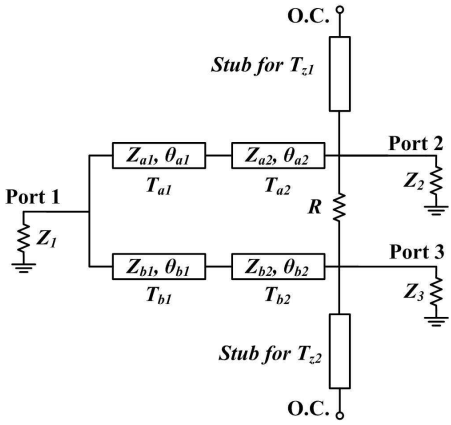

Figure 14. The proposed unequal-split power divider with one shunt open stub in each transmission path.

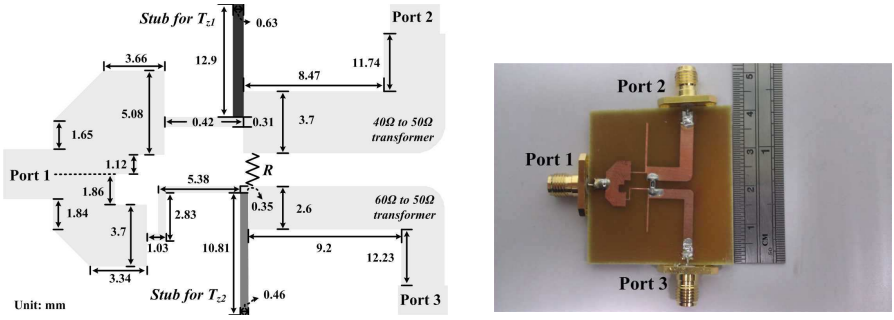

(a) (b)

Figure 15. (a) Layout and (b) photograph of the proposed unequal-split power divider with one shunt open stub in each transmission path.

required shunt-to-ground capacitor (C_1 or C_2). Here, the stubs for the two transmission zeros T_{z1} and T_{z2} are designed around 3.5 GHz and 4.5 GHz, respectively. Two $\lambda/4$ transformers must be added near the two output ports (Ports 2 and 3) for matching requirement because the termination resistors Z_2 and Z_3 are not equal to 50 Ω (the system impedance). Figure 15 shows the fabricated layout, and Figure 16 shows its simulated and measured results. The measured minimal insertion losses are 2.654 dB ($|S_{21}|$) and 4.401 dB ($|S_{31}|$), respectively, around the desired band. Therefore, the power ratio of measurement is 1.495. The measured maximal isolation ($|S_{32}|$) between

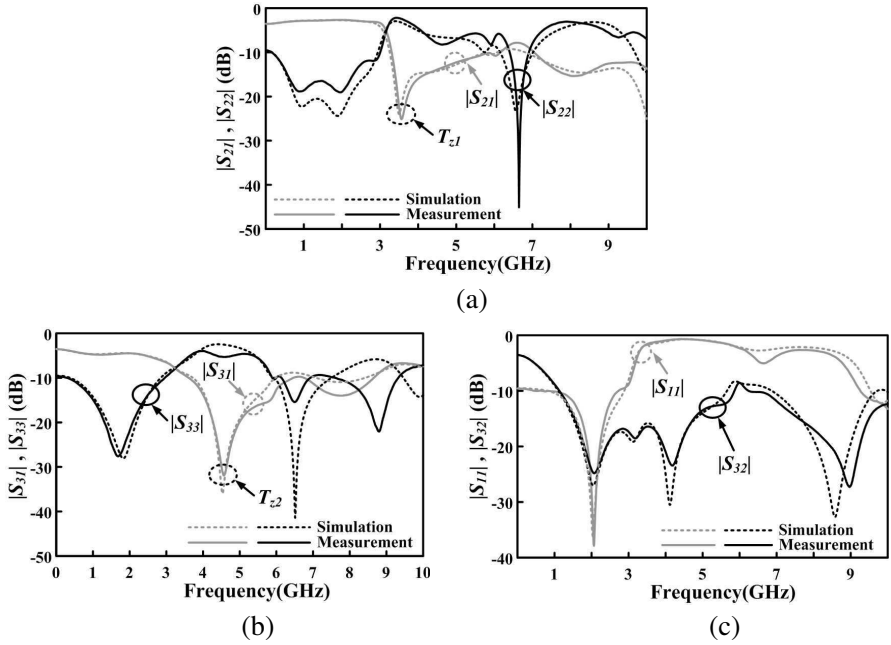

Figure 16. The measured and simulated scattering parameters of the proposed unequal-split power divider in Figure 15. (a) $|S_{21}|$ and $|S_{22}|$. (b) $|S_{31}|$ and $|S_{33}|$. (c) $|S_{11}|$ and $|S_{32}|$.

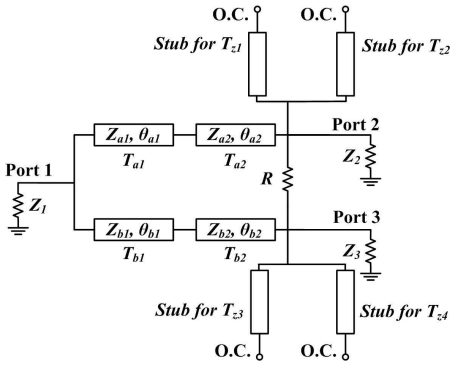

Figure 17. The proposed unequal-split power divider with two shunt open stubs in each transmission path.

two output ports is 24.5 dB around the desired band. This design exhibits remarkable rejection responses at approximately 3.5 GHz for $|S_{21}|$ and 4.5 GHz for $|S_{31}|$ due to the two shunt open stubs.

To confirm that the proposed unequal-split configuration can also produce two transmission zeros in each path, this study presents a final power divider with two open stubs in each transmission arm. Figure 17

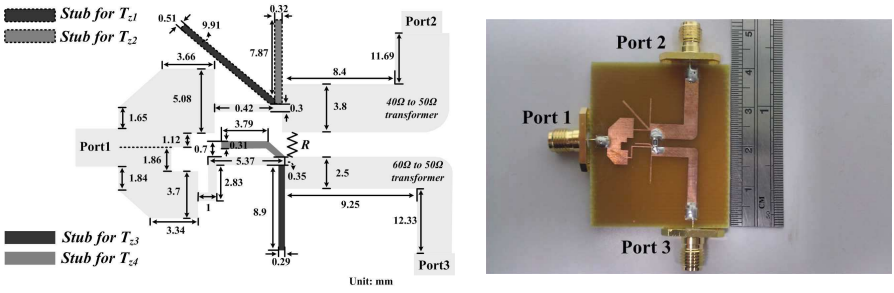

Figure 18. (a) Layout and (b) photograph of the proposed unequal-split power divider with two shunt open stubs in each transmission path.

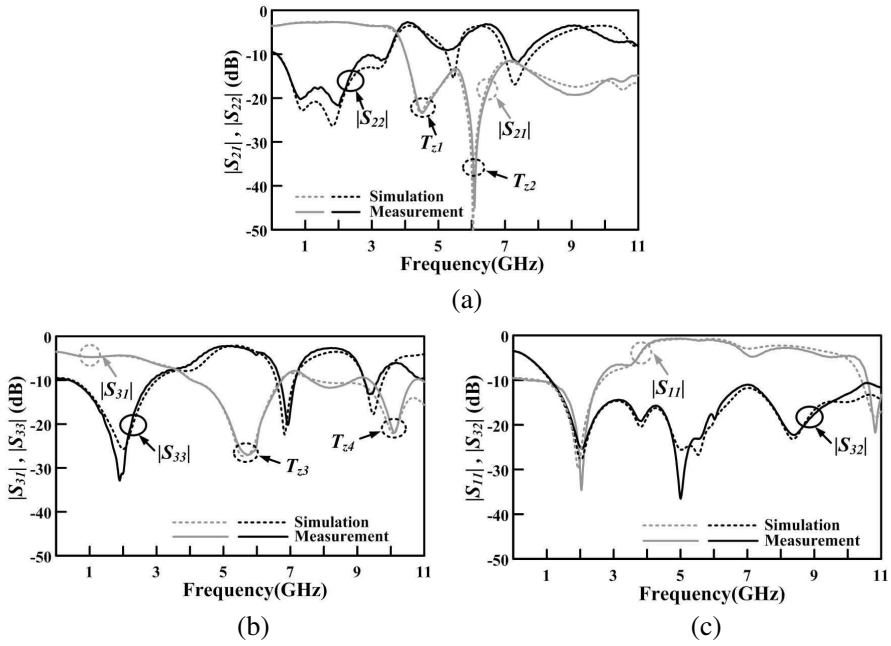

Figure 19. The measured and simulated scattering parameters of the proposed unequal-split power divider in Figure 18. (a) $|S_{21}|$ and $|S_{22}|$. (b) $|S_{31}|$ and $|S_{33}|$. (c) $|S_{11}|$ and $|S_{32}|$.

shows the equivalent-circuit model. All the design parameters and the center frequency are the same as the unequal-split divider (Figure 14) with the exception of implementing approach of shunt-to-ground capacitor in each path which is realized by two shunt open stubs in the proposed second unequal-split Wilkinson power divider. Here, the stubs for the four transmission zeros T_{z1}, T_{z2}, T_{z3}, and T_{z4} are designed at approximately 4.5 GHz, 6 GHz, 5.6 GHz, and 10 GHz, respectively. Two $\lambda/4$ transformers must be added near the two output ports to fulfill the matching requirement. Figure 18 illustrates the fabricated layout, and Figure 19 presents its simulated and measured results. The measured minimal insertion losses are 2.64 dB ($|S_{21}|$) and 4.4 dB ($|S_{31}|$), respectively, around the desired band. Therefore, the power ratio of measurement is 1.499. The measured maximal isolation ($|S_{32}|$) between two output ports is 26.2 dB around the desired band. This device also exhibits remarkable rejection responses at approximately 4.5 GHz/6 GHz for $|S_{21}|$ and 5.6 GHz/10 GHz for $|S_{31}|$ due to the four shunt open stubs.

7. CONCLUSION

This study presents new equal-split and unequal-split power dividers using stepped-impedance transmission lines and shunt-to-ground capacitors. Even- and odd-mode circuit analyses reveal that all design parameters in the proposed equal-split and unequal-split Wilkinson dividers can be determined. Therefore, using shunt open stubs to realize the shunt-to-ground capacitors make them possible to produce additional transmission zeros to improve the desired stopband responses. This study reports the successful fabrication of two microstrip equal-split and two unequal-split Wilkinson power dividers.

ACKNOWLEDGMENT

This study was supported by the National Science Council of Taiwan under Grant NSC 99-2221-E-390-007 and Grant NSC 100-2221-E-390-027.

REFERENCES

1. Pozar, D. M., *Microwave Engineering*, 2nd edition, Chapter 7, Wiley, New York, 1998.
2. Li, J. L., S. W. Qu, and Q. Xue, "Capacitively loaded Wilkinson power divider with size reduction and harmonic suppression,"

Microwave and Optical Technology Letters, Vol. 49, No. 11, 2737–2739, Nov. 2007.

3. Oraizi, H. and M. S. Esfahlan, "Miniaturization of Wilkinson power dividers by using defected ground structures," *Progress In Electromagnetics Research Letters*, Vol. 4, 113–120, 2008.
4. Shamsinejad, S., M. Soleimani, and N. Komjani, "Novel miniaturized Wilkinson power divider for 3G mobile receivers," *Progress In Electromagnetics Research Letters*, Vol. 3, 9–16, 2008.
5. He, J., B. Z. Wang, and W. Shao, "Compact power divider embedded with zigzag microstrip slow-wave structures," *Electronics Letters*, Vol. 45, No. 1, 62–63, Jan. 2009.
6. Zhang, Z., Y.-C. Jiao, S. Tu, S.-M. Ning, and S.-F. Cao, "A miniaturized broadband 4 : 1 unequal Wilkinson power divider," *Journal of Electromagnetic Waves and Applications*, Vol. 24, No. 4, 505–511, 2010.
7. Sedighi, S.-H. and M. Khalaj-Amirhosseini, "Compact Wilkinson power divider using stepped impedance transmission lines," *Journal of Electromagnetic Waves and Applications*, Vol. 25, No. 13, 1773–1782, 2011.
8. Wang, X. Y., J.-L. Li, and W. Shao, "Flexible design of a compact coupled-line power divider," *Journal of Electromagnetic Waves and Applications*, Vol. 25, No. 16, 2168–2177, 2011.
9. Huang, W., C.-J. Liu, Q. Chen, Y.-N. Li, X. Chen, and K.-M. Huang, "Compact unequal Wilkinson power dividers using planar artificial transmission lines," *Journal of Electromagnetic Waves and Applications*, Vol. 25, No. 16, 2201–2211, 2011.
10. Gupta, N., P. Ghosh, and M. Toppo, "A miniaturized Wilkinson power divider using DGS and fractal structure for GSM application," *Progress In Electromagnetics Research Letters*, Vol. 27, 25–31, 2011.
11. Li, X., Y.-J. Yang, L. Yang, S.-X. Gong, X. Tao, Y. Gao, K. Ma, and X.-L. Liu, "A novel design of dual-band unequal Wilkinson power divider," *Progress In Electromagnetics Research C*, Vol. 12, 93–100, 2010.
12. Park, M. J. and B. Lee, "A dual-band Wilkinson power divider," *IEEE Microwave Wireless Components Letters*, Vol. 18, No. 2, 85–87, Feb. 2008.
13. Yang, T., C.-J. Liu, L. Yan, and K.-M. Huang, "A compact dual-band power divider using planar artificial transmission lines for GSM/DCS applications," *Progress In Electromagnetics Research Letters*, Vol. 10, 185–191, 2009.

14. Wu, Y., Y. Liu, and S. Li, "An unequal dual-frequency Wilkinson power divider with optional isolation structure," *Progress In Electromagnetics Research*, Vol. 91, 393–411, 2009.
15. Wu, Y., Y. Liu, and S. Li, "Dual-band modified Wilkinson power divider without transmission line stubs and reactive components," *Progress In Electromagnetics Research*, Vol. 96, 9–20, 2009.
16. Wu, Y., Y. Liu, S. Li, C. Yu, and X. Liu, "Closed-form design method of an N-way dual-band Wilkinson hybrid power divider," *Progress In Electromagnetics Research*, Vol. 101, 97–114, 2010.
17. Shamaileh, K. A. A. and N. I. Dib, "Design of compact dual-frequency Wilkinson power divider using non-uniform transmission lines," *Progress In Electromagnetics Research C*, Vol. 19, 37–46, 2011.
18. Wu, Y., Y. Liu, Y. Zhang, J. Gao, and H. Zhou, "A dual band unequal Wilkinson power divider without reactive components," *IEEE Transactions Microwave Theory Techniques*, Vol. 57, No. 1, 216–222, Jan. 2009.
19. Li, J. C., J. C. Nan, X. Y. Shan, and Q. F. Yan, "A novel modified dual-frequency Wilkinson power divider with open stubs and optional isolation," *Journal of Electromagnetic Waves and Applications*, Vol. 24, 2223–2235, 2010.
20. Lin, Z. and Q.-X. Chu, "A novel approach to the design of dual-band power divider with variable power dividing ratio based on coupled-lines," *Progress In Electromagnetics Research*, Vol. 103, 271–284, 2010.
21. Huang, W., C.-J. Liu, L. Yan, and K.-M. Huang, "A miniaturized dual-band power divider with harmonic suppression for GSM applications," *Journal of Electromagnetic Waves and Applications*, Vol. 24, No. 1, 81–91, 2010.
22. Wang, X. H., L. Chen, X.-W. Shi, Y. F. Bai, L. Chen, and X.-Q. Chen, "Planar dual-frequency power divider using umbrella-shaped resonator," *Journal of Electromagnetic Waves and Applications*, Vol. 24, No. 5–6, 597–606, 2010.
23. Li, X., Y.-J. Yang, L. Yang, S.-X. Gong, T. Hong, X. Chen, Y.-J. Zhang, X. Tao, Y. Gao, K. Ma, and X.-L. Liu, "A novel unequal Wilkinson power divider for dual-band operation," *Journal of Electromagnetic Waves and Applications*, Vol. 24, No. 8–9, 1015–1022, 2010.
24. Dai, G. L. and M. Y. Xia, "A dual-band unequal Wilkinson power divider using asymmetric coupled-line," *Journal of Electromagnetic Waves and Applications*, Vol. 25, No. 11–12, 1587–1595, 2011.

25. Li, B., X. Wu, N. Yang, and W. Wu, "Dual-band equal/unequal Wilkinson power dividers based on coupled-line section with short-circuited stub," *Progress In Electromagnetics Research*, Vol. 111, 163–178, 2011.
26. Yang, J., C. Gu, and W. Wu, "Design of novel compact coupled microstrip power divider with harmonic suppression," *IEEE Microwave Wireless Components Letters*, Vol. 18, No. 9, 572–574, Sep. 2008.
27. Yi, K. H. and B. Kang, "Modified Wilkinson power divider for nth harmonic suppression," *IEEE Microwave Wireless Components Letters*, Vol. 13, No. 5, 178–180, May 2003.
28. Tu, W. H., "Compact Wilkinson power divider with harmonic suppression," *Microwave and Optical Technology Letters*, Vol. 49, No. 11, 2825–2827, Nov. 2007.
29. Fan, F., Z. H. Yan, and J. B. Jiang, "Design of a novel compact power divider with harmonic suppression," *Progress In Electromagnetics Research Letters*, Vol. 5, 151–157, 2008.
30. Cheng, K. K. M. and W. C. Ip, "A novel power divider design with enhanced spurious suppression and simple structure," *IEEE Transactions Microwave Theory Techniques*, Vol. 58, No. 12, 3903–3908, Dec. 2010.
31. Ahn, H. R. and I. Wolff, "General design equations, small-sized impedance transformers, and their application to small-sized three-port 3-dB power dividers," *IEEE Transactions Microwave Theory Techniques*, Vol. 49, No. 7, 1277–1288, Jul. 2001.
32. Chen, H. and Y.-X. Zhang, "A novel compact planar six-way power divider using folded and hybrid-expanded coupled lines," *Progress In Electromagnetics Research*, Vol. 76, 243–252, 2007.
33. Kim, J. G. and G. M. Rebeiz, "Miniature four-way and two-way 24 GHz Wilkinson power dividers in 0.13 μm CMOS," *IEEE Microwave Wireless Components Letters*, Vol. 17, No. 9, 658–660, Sep. 2007.
34. Parad, L. I. and R. L. Moynihan, "Split-tee power divider," *IEEE Transactions Microwave Theory Techniques*, Vol. 13, No. 1, 91–95, Jan. 1965.
35. Naghavi, A. H., M. Tondro Aghmiyouni, M. Jahanbakht, and A. A. Lotfi Neyestanak, "Hybrid wideband microstrip Wilkinson power divider based on lowpass filter optimized using particle swarm method," *Journal of Electromagnetic Waves and Applications*, Vol. 24, No. 14–15, 1877–1886, 2010.

36. Qaroot, A. M. and N. I. Dib, "General design of N-way multi-frequency unequal split Wilkinson power divider using transmission line transformers," *Progress In Electromagnetics Research C*, Vol. 14, 115–129, 2010.
37. Peters, F. D. L., D. Hammou, S. O. Tatu, and T. A. Denidni, "Modified millimeter-wave Wilkinson power divider for antenna feeding networks," *Progress In Electromagnetics Research Letters*, Vol. 17, 11–18, 2010.
38. Kim, K., J. Byun, and H.-Y. Lee, "Substrate integrated waveguide Wilkinson power divider with improved isolation performance," *Progress In Electromagnetics Research Letters*, Vol. 19, 41–48, 2010.
39. Zhou, B., H. Wang, and W.-X. Sheng, "A modified UWB Wilkinson power divider using delta stub," *Progress In Electromagnetics Research Letters*, Vol. 19, 49–55, 2010.
40. Chiang, C. T. and B.-K. Chung, "Ultra wideband power divider using tapered line," *Progress In Electromagnetics Research*, Vol. 106, 61–73, 2010.
41. Qaroot, A. M., N. I. Dib, and A. A. Gheethan, "Design methodology of multi-frequency unequal split Wilkinson power dividers using transmission line transformers," *Progress In Electromagnetics Research B*, Vol. 22, 1–21, 2010.
42. Huang, S., X. Xie, and B. Yan, "K band Wilkinson power divider based on a taper equation," *Progress In Electromagnetics Research Letters*, Vol. 27, 75–83, 2011.
43. Wu, Y. and Y. Liu, "An unequal coupled-line Wilkinson power divider for arbitrary terminated impedances," *Progress In Electromagnetics Research*, Vol. 117, 181–194, 2011.
44. Wang, D., H. Zhang, T. Xu, H. Wang, and G. Zhang, "Design and optimization of equal split broadband microstrip Wilkinson power divider using enhanced particle swarm optimization algorithm," *Progress In Electromagnetics Research*, Vol. 118, 321–334, 2011.